JACS
JOURNAL OF THE AMERICAN CHEMICAL SOCIETY

ARTICLE

pubs.acs.org/JACS

Ultrafast Hybridization Screening in Fe^{3+} Aqueous Solution

Stephan Thürmer,[†] Robert Seidel,[†] Wolfgang Eberhardt,[†] Stephen E. Bradforth,[‡] and Bernd Winter*[,†]

[†]Helmholtz-Zentrum Berlin für Materialien und Energie, and BESSY, Albert-Einstein-Strasse 15, D-12489 Berlin, Germany

[‡]Department of Chemistry, University of Southern California, Los Angeles, California 90089, United States

Supporting Information

ABSTRACT: We report here on the electron binding energies and ultrafast electronic relaxation of the $Fe^{3+}(aq)$ complex in $FeCl_3$ aqueous solution as measured by soft X-ray photoelectron (PE) spectroscopy from a vacuum liquid microjet. Covalent mixing between the 3d valence orbitals of the iron cation and the molecular orbitals of water in the ground-state solution is directly revealed by spectroscopy of the highest partially occupied molecular orbitals. Valence PE spectra, obtained for photon energies near the iron 2p absorption edge, exhibit large resonant enhancements. These resonant PE features identify 3d−O2p transient hybridization between iron and water-derived orbitals and are an indication of charge transfer within the electronically excited $Fe^{3+}(aq)^*$ complex. Charge transfer from water to iron is also revealed by the 2p core-level PE spectrum, and the asymmetric peak shape additionally identifies the characteristic multiplet interactions in the 2p core-hole state. The electronic structure of water molecules in the first hydration shell is selectively probed by Auger decay from water molecules, at excitation energies well below the O1s absorption edge of neat water. These experiments lay the groundwork for establishing resonant PE spectroscopy for the study of electronic-structure dynamics in the large family of transition metal (aqueous) solutions.

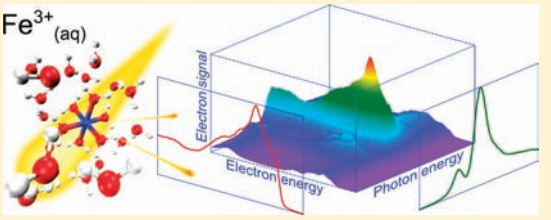

INTRODUCTION

Approximately 60 years after the first report of light-induced electron transfer excitation in Fe^{3+} aqueous solution,[1] experimental X-ray-based spectroscopic techniques[2] are becoming available for the study of electronic-structure interactions between solute and water solvent in bulk aqueous solution, on the microscopic level. That includes both the direct interactions with the water molecules in the first solvation shell as well as longer-range effects from more distant water molecules. The nature of the solute−water interaction is of fundamental importance, relevant for multiple disciplines such as electro- and radiochemistry, electronic-structure theory, chemistry, and biology, including the crucial role of the first-row 3d transition-metal (TM) cations exhibiting biological functionality. Yet, to date, even the arguably most-important electronic structure quantity, the electron binding energy (BE) of the 3d-derived highest (partially) occupied molecular orbitals, has been measured only for Ru^{2+} and Mn^{2+} in aqueous solution.[3,4] Knowledge of the lowest ionization energy is crucial for understanding charge transfer and chemical reactivity. With the help of the measured vertical ionization energies for different charge states (2^+, 3^+), we can also experimentally determine reorganization energies, associated with the rearrangement of water molecules in the first solvation shell upon oxidation/reduction of the metal cation. Core-level and resonant PE spectra from any TM aqueous solution have, so far, not been reported, except for a very recent work from $NiCl_2$ aqueous solution,[5] which, however, does not provide any spectral interpretation.

In addition to the previous experimental hurdles in conducting PE studies from aqueous solutions,[6,7] the interpretation of PE spectra from TM ions in water is quite complex, complicated by electronic-correlation effects and by charge transfer between solvent (ligand) and metal cations, and vice versa (denoted LMCT and MLCT, respectively) in both the ground and the excited states. Correlation interactions in the presence of a core hole lead to a series of final states with different symmetries and energies, the final-state multiplet.[8] Valence charge transfer from ligand to metal cation, accompanying core-hole creation, can be very efficient, and the PE spectra may be even dominated by contributions from screened rather than unscreened states.[9] The creation of a core hole is the initial step of any of the X-ray spectroscopy techniques discussed here. In the case of TMs (we here investigate 2p core-excitations), the absorption of an X-ray photon either (i) excites a core-electron into an empty or partially filled 3d valence electronic state (X-ray absorption;[8] XA), or (ii) a photoelectron is directly emitted into vacuum (photoelectron emission;[9] PE), where it is observable at a certain kinetic energy (KE). In both cases, the particular spectral structure is strongly influenced by 3d−2p electron correlations, and these need to be distinguished from contributions connected with mere ground-state electronic properties, such as solute−water mixed state energies.

Here, we focus entirely on experimental electron X-ray spectroscopy, specifically on the measurement of the kinetic energies of electrons emitted into vacuum from an aqueous solution upon irradiation by monochromatic soft X-rays.

Received: January 11, 2011
Published: July 14, 2011

These are either direct photoelectrons or electrons created in some second-order process, usually involving Auger decay. The valence photoelectron spectrum, when measured at photon energies resonant with the TM-cation $2p_{3/2,1/2}$ absorption ($L_{3,2}$ edge), is called the 2p resonant PE (RPE) spectrum,[8−10] and sometimes the method is referred to as de-excitation electron spectroscopy (DES).[11] Large intensity increase of certain distinct spectral features as compared to the off-resonant PE spectra can occur, and these changes contain crucial information on how the electronically excited Fe^{3+}(aq) complex relaxes. These electronic relaxations occur within the few-femtosecond lifetime typical for core holes,[12,13] as they are faster than the competing radiative decays, and the RPE spectra thus track the very early electron dynamics, which may be as fast as attoseconds.[14] The unique spectral specificity of RPE makes the method far more powerful than common XA spectroscopy, which measures total fluorescence yield (TFY) or total electron yield (TEY).[15,16] Yet, such integrated XA spectra are sometimes helpful and are easier to calculate.[8] In fact, for the present case of TM cations in water, we find the comparison with XA spectra from TM-oxides to be very rewarding. In our studies, we obtain total and partial electron yield-XA spectra simply from signal integration of the measured PE spectra over a suitable electron KE range. Specifically, partial electron yield (PEY) spectra are obtained by plotting the total signal increase in the valence RPE spectra when sweeping the photon energy across the iron 2p resonance. In this way, specific core-hole excited states can be precisely correlated with specific RPE spectral features, allowing identification of the electronic configuration of the final state. This enables us to distinguish between single-hole and multi-hole (Auger) final states, which is crucial for quantifying electron transfer between H_2O and the metal ion in the ground and excited states.

EXPERIMENTAL SECTION

Photoemission measurements were performed from a 15 μm-sized vacuum liquid jet[6,7,17] at the soft-X-ray U41 PGM undulator beamline of BESSY II, Berlin. The jet velocity was approximately 100 ms^{-1}, and the jet temperature was 6 °C. Electrons were detected normal to both the synchrotron-light polarization vector and the flow of the liquid jet. A 100 μm diameter orifice that forms the entrance to the hemispherical electron energy-analyzer is at approximately 0.5 mm distance from the liquid jet, a short enough distance to ensure that detected electrons have not suffered from inelastic scattering with water gas-phase molecules around the small-sized liquid jet.[6] At operation conditions, the pressure in the interaction chamber was about 1.5×10^{-4} mbar. The energy resolution of the U41 beamline is better than 200 meV at the incident photon energies used here, and the resolution of the hemispherical energy analyzer is constant with kinetic energy (about 200 meV, at 20 eV pass energy). The small focal size, 23×12 μm^2, of the incident photon beam allows for matching spatial overlap with the liquid microjet, reducing the gas-phase contributions of the measured spectra to less than 5%. The aqueous solutions were prepared using deionized water, and the $FeCl_3$ ($Fe(NO_3)_3$) salt was of 98% purity (Sigma Aldrich). Concentrations of 0.5, 1.0, and 1.5 molal were studied here, although our focus is on 1 *m*. HCl (0.1 *m*) was added to the as-prepared solutions to reduce the pH to <1, which suppresses hydroxo-complex formation.[18,19] Comparative measurements from $Fe(NO_3)_3$ aqueous solutions, also with 0.1 *m* HCl added, showed no noteworthy counteranion effects. Note that the hexa-aqua structure is unfavorable in water at these concentrations; in the dominant configuration, at least one of the six water molecules will be substituted by the respective anion of the salt used.[19,20] Here, this configuration is denoted aqua^{-1} complex, and when referring to octahedral coordination it is implied that not all six ligands are H_2O. A detailed consideration of speciation and how it affects our RPE spectra will be presented below.

RESULTS AND DISCUSSION

Figure 1 displays valence and core-level PE spectra from 1 *m* $FeCl_3$ aqueous solution measured at some off-resonance photon energies. The valence PE spectra of Figure 1A were obtained at 201 and 703 eV photon energies, where the latter is somewhat below the 2p absorption edge of the iron cation. Both spectra are dominated by electron emission from water orbitals, $1b_1$, $3a_1$, $1b_2$, and $2a_1$, which occur at the same electron binding energies as for neat liquid water.[17] Chloride 3p and 3s energies are exactly as reported in our previous work on inorganic aqueous solutions.[21] Observed large differences in intensity of the chloride 3p feature in the two different traces arise from different ionization cross sections at the two photon energies. The small intensity near the energy of the Cl3s peak in the upper spectrum is due to Cl^- spectator Auger-electron emission and is associated with chloride 2p excitation into the lowest charge-transfer-to-solvent (CTTS) state. This transition happens to occur at 201 eV.[22] The valence-signal contributions from Fe^{3+} 3d-derived orbitals, which are small, must yet be evaluated by spectral peak fitting, which can be done with high accuracy because the spectra of neat water and of chloride aqueous solution are exactly known. Individual spectral contributions inherent to the iron in solution can thus be represented by the series of Gaussians, as shown in Figure 1A. Gaussian peak positions and widths are the same as determined previously for water and alkali aqueous solutions,[17,21] and a very good total fit to the experimental PE spectrum is obtained when including two additional unconstrained Gaussians at 10.2 and 8.9 eV BE. These are the iron $3d^5$-derived energies and can be thought of to represent the e_g and t_{2g} orbitals, which are both singly occupied in the high-spin ground state produced by the octahedral oxygen ligand field imposed by the hydrating water molecules, analogous to ligand-field splitting in iron-oxide.[8,23−25] Qualitatively, the observed t_{2g}/e_g PE signal-ratio of approximately 3:2 (Figure 1A) would be in agreement with the 3-electron/2-electron occupancy in a high-spin configuration. The energy difference between the lowest-energy iron peaks of 10 Dq = 1.3 eV is somewhat smaller than that determined from optical spectra (10 Dq = 1.5 eV),[20] and possibly results from small undetected peak shift of the water $1b_1$ orbital in the PE spectra. Our description of the iron-derived energies is simplified, though, as it neglects hybridization between unscreened and screened electronic ground-state configurations. These effects do play a crucial role in core-level ionization of (solid phase) transition-metal oxides.[24] To what extent this also applies for aqueous solutions will be discussed below along with the iron 2p PE spectra and the corresponding resonant valence PE spectra. In fact, the latter spectra are also useful in identifying metal-derived peaks with very low signal intensities at nonresonant excitation, as is the case for the Fe^{3+} peaks in the valence spectrum. We will later use these two energy values to assign specific X-ray transitions to the peaks of the Fe^{3+} 2p(aq) (L-edge) XA spectrum, and we are particularly interested to find whether the same partially filled 3d levels are populated by O1s (K-edge) absorption.

The O1s and Fe^{3+} 2p core-level PE spectra from the $FeCl_3$ aqueous solution are shown in Figure 1B and C. The O1s spectrum exhibits one single broad peak at the same energy of

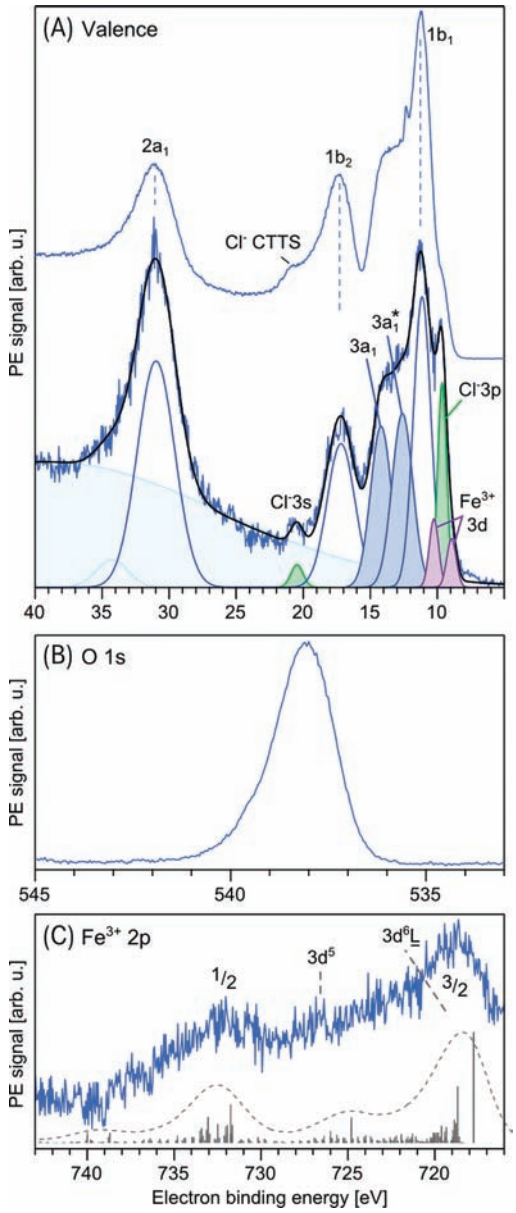

Figure 1. Off-resonant PE spectra from 1 m $FeCl_3$ aqueous solution. (A) Valence PE spectra measured at 201.3 (top) and 703.4 eV (bottom) photon energy. The Gaussian fits to the bottom spectrum identify the contributions from the individual orbitals. For fitting the water $3a_1$ peak, we have used two peaks as discussed in ref 17. Filled peaks coincide with the energies at which resonant enhancement is observed. (B) Oxygen 1s PE spectrum measured at 603 eV photon energy. (C) Fe^{3+} 2p PE spectrum measured at 925.7 eV photon energy. The peaks labeled 1/2 and 3/2 correspond to the screened $\underline{2p}_{1/2}3d^6\underline{L}$ and $\underline{2p}_{3/2}3d^6\underline{L}$ final states. Stick marks present the calculated multiplet relative energy positions for Fe^{3+}, which is included here to show the origin of the asymmetric peak shape and width. For the calculations, we have used 10 Dq = 1.5, Δ = 5.5, U_{dd} = 5.5, U_{cd} = 8; adapted from Fe_2O_3.[38] Label $3d^5$ indicates the suggested energy position of the $\underline{2p}_{3/2}3d^5$ unscreened final state.

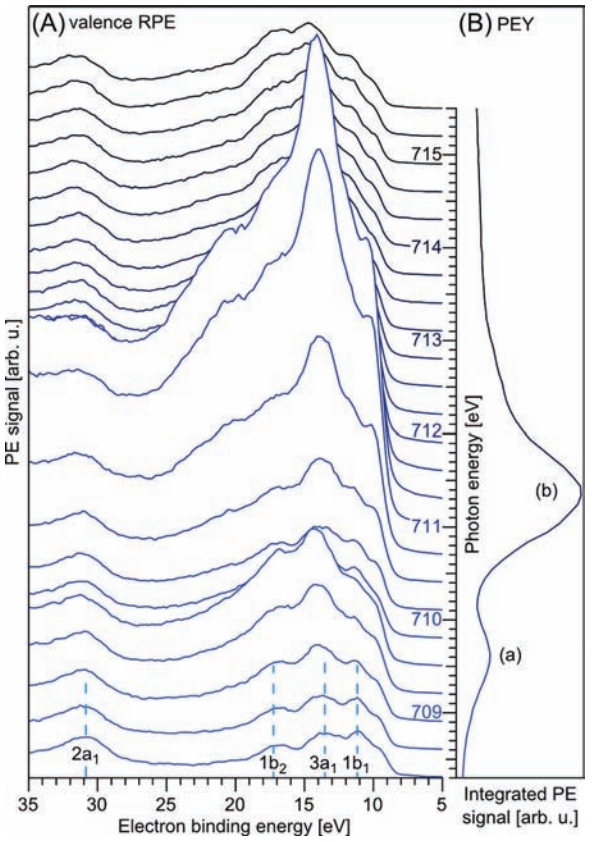

Figure 2. (A) Iron 2p valence RPE-spectra from 1 m $FeCl_3$ aqueous solution for photon energies at and around the Fe^{3+} L_3 XA edge. (B) Fe^{3+} $2p_{3/2}$ PEY-XA spectrum as obtained by signal integration of the respective RPE spectra, shown left. Label (a) is the XA prepeak, and (b) is the corresponding main peak.

538.1 eV, and with peak shape identical to that in neat liquid water.[26] Chemical BE shifts associated with the iron–water interaction stay thus undetected within approximately 200 meV experimental uncertainties, at least for this relatively small ratio of shell-to-bulk water molecules. However, the effect of the metal cation on the electronic structure of water can be sensitively detected through changes of O1s valence RPE spectra, when the excitation photon energy is on resonance with the O1s XA energy of first-shell water molecules (see below). The Fe^{3+} $2p_{3/2,1/2}$ core-level PE spectra from the solution, Figure 1C, are dominated by electronic multiplet and screening effects associated with the core hole produced in the photoemission process.

The main peaks at 719 and 732 eV BE, as calibrated by the O1s energy of liquid water,[26] are the $\underline{2p}_{3/2}3d^6\underline{L}$ and $\underline{2p}_{1/2}3d^6\underline{L}$ charge-transfer final states and correspond to the iron 2p core-hole screened by a ligand electron. $\underline{L}$, $\underline{2p}$ denote a hole in the water ligand and a hole in the 2p level, respectively. PE charge-transfer peaks are well-known for TM-oxides, and the present assignment is based on comparison with 2p PE spectra from crystalline α-Fe_2O_3 (hematite),[8,25,27] which exhibit a similar overall spectral shape. Note that energies reported here are with respect to vacuum, whereas the oxide literature usually refers to the Fermi energy or to some other reference energy. Comparison with hematite is useful because it is arguably the best solid-state analogue of Fe^{3+} in water. In both phases, the Fe^{3+} cation is coordinated by six oxygens, giving rise to octahedral symmetry, and the Fe–O distances are almost identical. Hence, ligand-field splitting of the atomic $3d^5$ configuration should lead to rather similar e_g and t_{2g} high-spin state energies, if we neglect hybridization. Yet ligand-to-metal charge transfer ought to be different in aqueous solutions and oxides, which is indeed the case as we will

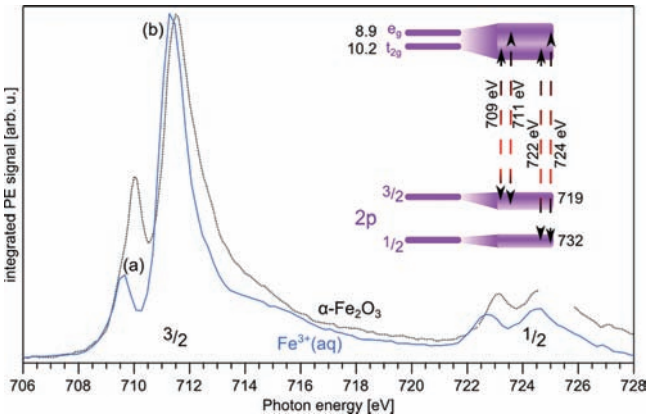

Figure 3. Comparison of the iron $L_{3,2}$-edge PEY-XA spectra from 1 m $FeCl_3$ aqueous solution (blue) and from α-Fe_2O_3 crystalline iron oxide (black-dotted line; from ref 25). The solution L_3 spectrum is the same as in Figure 2B. Inset: XA transitions from the 2p core level to the 3d states.

demonstrate below by our RPE measurements. Probably, a first indication is the surprisingly low Fe^{3+} 2p PE signal level from solution, which can neither be explained on the basis of atomic photoionization cross sections[28] nor by surface depletion of the metal cation. The same low 2p PE signal was found for shorter and larger probing depth, where we have adjusted the kinetic energy of the photoelectrons by suitable choice of photon energy.[29] The most reasonable explanation for the unexpectedly low 2p signal intensity is the large distribution of hydration configurations in the fluxional solution network, primarily leading to different water−metal distances. Because of the resulting variation of electronegativity of the ligand, charge-transfer rates and formal charge state will alter, and combined with the multiplet effects, which are specific for each configuration, relative energy changes can be considerable. As a consequence, spectral contributions are more spread-out than for the rigid Fe^{3+} sites in the octahedral oxygen configuration of oxides. Unfortunately, because of the low 2p signal (low signal/noise ratio), unscreened states $\underline{2p}_{3/2}3d^5$ and $\underline{2p}_{1/2}3d^5$ can be barely detected; in hematite, they occur at approximately 8 eV higher BE than the respective main peaks.[25] Part of the difficulty in assigning unscreened states is due to the large asymmetry of 2p PE peaks toward the high-BE side, which primarily arises from multiplet effects such as 2p−3d exchange interaction.

We now explore the ultrafast relaxation processes of the core-excited Fe^{3+} in aqueous solution in detail and determine the electronic states involved. We analyze the respective RPE spectra on the basis of experimental and calculated XA spectra from crystalline TM oxides. Figure 2 (left) shows the series of RPE valence spectra from 1 m $FeCl_3$ aqueous solution, where the photon energy has been tuned across the $2p_{3/2}\rightarrow$3d resonance. The lowest photon energy used here was 708.3 eV, which produces a spectrum (bottom-most tier) similar to the 703 eV off-resonant PE spectrum of Figure 1A. Large nonuniform signal enhancement is observed, amounting to an approximately 10× overall signal increase within the displayed valence region, when the photon energy is 711.5 eV. Most noticeable is the growth of a strong peak at constant electron binding energy position, coincident with the emission from the water $3a_1$ orbital. This orbital has mixed O2p, O2s, and H1s bonding character and is oriented along the hydrogen donor-bond axis in liquid water. Contributions from Auger electrons (3d3d; refill of the 2p hole by one 3d electron and emission of a second 3d electron) are identified by the constant KE peaks; these peaks move in the BE presentation of Figure 2. A plot of the integrated PE signal, for each individual photon energy, yields the iron L_3-edge (Fe^{3+} $2p_{3/2}$) partial-electron yield XA spectrum and is shown at the right-hand side of Figure 2. We can make the analogous measurements at the Fe^{3+} $2p_{1/2}$ resonance. The resulting full $L_{3,2}$-edge PEY-XA spectrum of Fe^{3+} aqueous solution is shown in Figure 3; here, the L_3 part is identical to the one in Figure 2.

The observed L_3 XA double-peak structure (Figure 3), with a small peak (a) and a large peak (b), is very similar to that in the L_3-edge XA spectrum of crystalline α-Fe_2O_3,[24] which is also shown for comparison. From the extensive literature on iron-oxides[8] and other ligands,[30,31] it is well-known that in particular this prepeak structure is a sensitive spectral fingerprint of $3d^5$ high-spin ground-state configuration in an octahedral ligand field. The (b)/(a) signal ratio is in fact a nearly quantitative measure of the amount of d-character of unoccupied valence orbitals of the metal; the energy difference, (b) − (a), to first approximation reflects the ligand field splitting (10 Dq), which determines the e_g and t_{2g} energies. In the light of similar symmetry of the iron ion in the two different environments (water vs oxide), large similarity of the L_3 XA spectra from Fe^{3+} in aqueous solution and iron-oxide may hence not be too surprising. It shows, however, that from the XA spectrum alone we can barely infer the subtle electronic-structure differences between the Fe^{3+} when surrounded by six H_2O molecules versus six oxygen atoms in crystalline Fe_2O_3. We obviously need further experimental data to reveal, for instance, the higher charge density at the cation due to the shared oxygens between metal cations. This is where RPE measurements come into play, providing more clear insight into charge-transfer processes and into the electronic configurations involved. Implementation of charge transfer in ligand-field multiplet theory has been described in the literature, but these corrections usually have small and yet distinct effects.[8] In general, multiplet theory reproduces experimental XA spectra from TM oxides fairly accurately, capturing spin state and ligand effects.[8] One important observation from Figure 3 is that the differences between the $2p_{3/2}$ XA spectra from solution and from oxide occur for excited states where charge transfer is expected to contribute.[8] This suggests less charge transfer from the ligand to the iron cation in solution, and yet detailed theoretical treatment is required to quantify charge transfer, including electron donation and back-donation between the different electronic ground-state configurations (see Figure 5A).

Before discussing the RPE spectra in greater detail, it is instructive to compare the measured XA (transition) energies and the BEs from the PE spectra. We find that the respective energy differences between the L_3 absorption energies at 709/711 eV (Figure 3) and the $2p_{3/2}$ BE at 719 eV (Figure 1A) match the measured 10.2 and 8.9 eV BEs of the mixed iron−water partially filled 3d-derived levels. This also holds for the L_2 edge, in which case absorption maxima are at 722/724, and 732 eV is the $2p_{1/2}$ BE. That is an important experimental result, suggesting that the iron X-ray transitions are indeed $2p\rightarrow e_g$, t_{2g}, as depicted in the inset of Figure 3.

With the lack of theoretical calculations of RPE spectra from aqueous solutions, we pursue two different ways in an attempt to extract and to explain the additional new information contained in these spectra. One involves a comparison with the reported TM-oxide data, and the other is a more speculative (but intuitive)

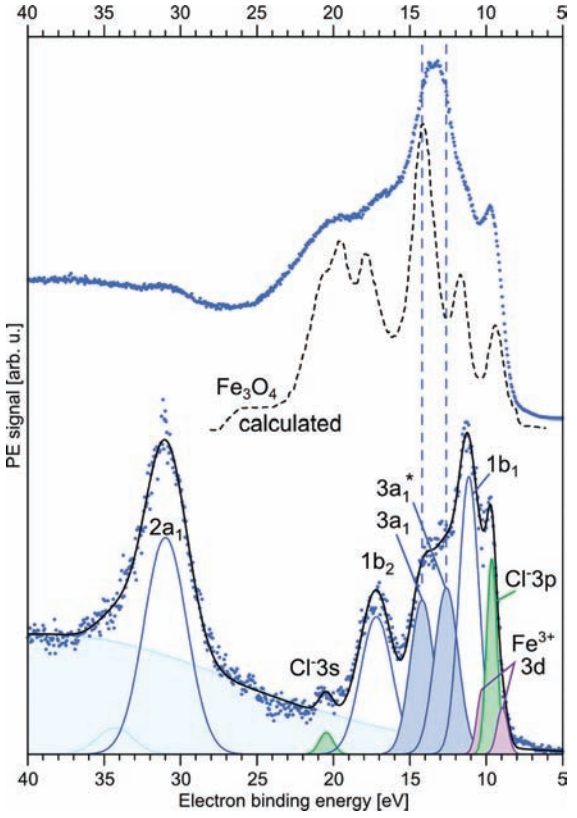

Figure 4. Comparison of the experimental iron 2p valence RPE spectrum from 1 m $FeCl_3$ aqueous solution (top), measured at 711 eV photon energy, and the calculated RPE spectrum of the Fe^{3+} site in Fe_3O_4 crystal (center; from ref 32). The bottom spectrum is the off-resonant valence PE spectrum, measured at 703 eV photon energy.

approach trying to explain specific spectral changes involving concepts of transient hybridization. In the first approach, we compare the measured spectra from iron solution with computed RPE spectra from Fe_3O_4 (magnetite), containing Fe^{3+} in octahedral-symmetry oxygen configuration as a minority structure. Analogous work for Fe_2O_3, which would be more useful, has not been reported. The top and bottom tiers of Figure 4 reproduce the 711 eV RPE spectrum and the 703 eV off-resonant PE spectrum from 1 *m* $FeCl_3$ aqueous solution of Figures 2 and 1, respectively. The center tier is reproduced from ref 32 and shows the calculated RPE spectrum for the Fe^{3+} site in magnetite; the spectrum has been shifted such that the prominent features line up with the experimental spectrum. Although this is a crude comparison, there is considerable overall agreement between the experimental solution RPE and the calculated oxide RPE spectrum. Obviously, the theoretical models for TM oxides do fairly well capture several essential electronic-structure properties in the ground and in the RPE final state of the solution, at least qualitatively. It is not intended here to discuss the (oxide) RPE-spectrum calculations and their implications in exact detail, but we do point out a few aspects that promote our understanding of the experimental RPE spectra from solution.

The overall structure of the computed RPE spectrum from hematite has been explained by strong ligand-to-iron charge transfer involving Fe 3d−O 2p hybridization. As a result, some of the $3d^5\underline{L}$ final states are coupled with the $3d^4$ states and are pushed out to low binding energies. This leads to the three

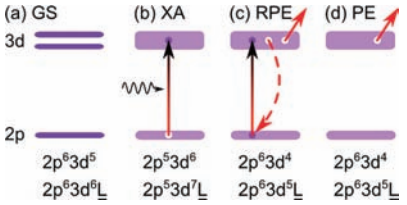

Figure 5. Energy-level schemes depicting the iron-derived 3d, 2p electronic configurations of Fe^{3+} aqueous solution: (a) ground state, (b) L-edge XA intermediate state, (c) 2p RPE final state, (d) 2p PE final state. Energy differences between unscreened (L) and screened ($\underline{L}$) states have been omitted.

structures in the calculated spectrum consisting of a rather broad feature centered around 19 eV, a single peak at 14 eV, and peaks below 12 eV. The 14 eV single peak is assigned to the nonbonding $3d^5\underline{L}$ final state, while the peaks below 12 eV and near 19 eV result from the $3d^4/3d^5\underline{L}$ bonding and antibonding multiplets, respectively.[32] Obviously, the resonance process enhances the intensities of photoelectrons corresponding to the final-state configurations of $3d^4$ and $3d^5\underline{L}$.[32] Electronic configurations and their energies relevant for the present discussion are depicted in the energy-level schemes of Figure 5, which also contain the respective illustration for the intermediate states reached in XA. From the similarity of valence RPE and of 2p PE spectra from iron solution and iron oxide, we conclude that charge transfer plays also a crucial, but smaller role in solution. Our data show no evidence for charge-back-donation, but clearly quantification of any of these effects must await dedicated theoretical calculations of RPE spectra from aqueous solution. Differences in charge transfer likely result from the stabilization of the water hydrogen-bonded network, where charge transfer away from the water competes with maintaining hydrogen-bonding interactions between water molecules.

In the following, a more qualitative but challenging explanation of the RPE spectra from iron solution is presented. When comparing the experimental on- and off-resonant iron-2p RPE spectra from 1 *m* $FeCl_3$ aqueous solution, top and bottom tiers of Figure 4, one finds that the main signal enhancements at 13 and 14.5 eV BE can be formally explained entirely by the increase of the electron-emission intensity from water $3a_1$ (indicated by dashed vertical lines). Also, the signal from 3d-derived e_g and t_{2g} states is enhanced, which can be seen when comparing with the almost invisible intensity of the water $2a_1$ peak at resonant excitation. The observed resonant enhancement indicates the involvement of these electrons in screening the core-hole excited state.[11] Accordingly, the large enhancement that leads to the relatively narrow band at the $3a_1$ energy suggests a transient ultrafast hybridization between 3d and $3a_1$ orbitals in the core-excited state, enabling water-to-cation charge transfer. In the core-excited state, the 3d and $3a_1$ states are close in energy as a result of the energy shift of the 3d-level due to Coulomb interaction with the 2p core hole. Auger decay of that transient mixed state (analogous to $3d^5\underline{L}$) leads to the same final state reached in direct ionization of $3a_1$ (compare Figure 5); interference of the identical final states gives rise to the resonant enhancement. The picture described here is the formal analogue to RPE from metals,[9,33−35] albeit the screening is typically via sp and d electrons in the latter systems.

Our studies of the electronic-structure interactions between the Fe^{3+} cation and its surrounding water molecules would be incomplete without consideration of the corresponding

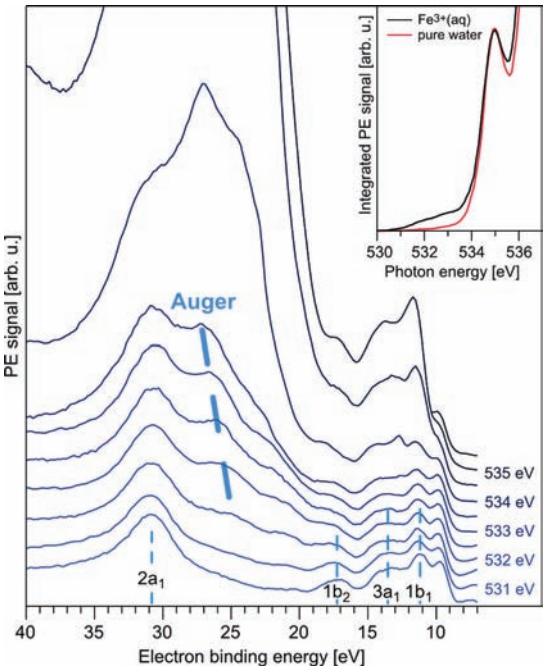

Figure 6. O1s RPE spectra from 1 m $FeCl_3$ aqueous solution for photon energies corresponding to the O1s absorption of water molecules of the first hydration shell of Fe^{3+}. Inset: O1s PEY-XA spectrum (black) as obtained by signal integration of the respective RPE spectra of the main figure. The corresponding spectrum from neat water is shown for comparison (red).

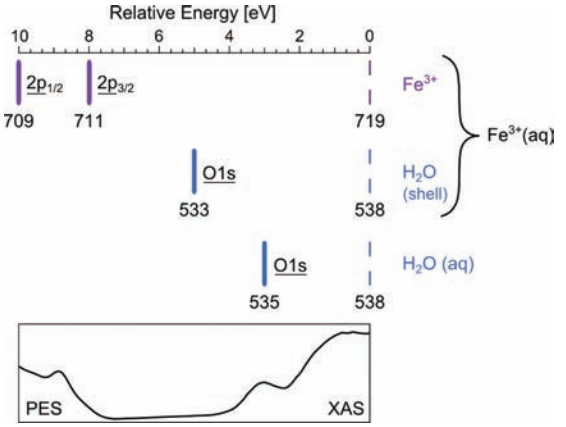

Figure 7. Relative difference between ionization energy (onset energy for electron emission into vacuum) and core excited states. States are shown for Fe^{3+} 2p and O1s for water both in the hydration shell and in bulk water.

oxygen-1s RPE spectra. This in fact brings up the very important, and by no means trivial, questions of whether electron excitation from water O1s and Fe^{3+} 2p involves the same unoccupied orbital, and how these two spectroscopic profiles connect. To this end, we have measured oxygen K-edge (valence) RPE spectra from 1 *m* $FeCl_3$ aqueous solution; see Figure 6. Note that the photon energies for resonant excitation of water in the $Fe^{3+}\cdot aqua^{-1}$ complex start around 532 eV, that is, well below the onset of water absorption, which only sets in at approximately 534 eV. This can be best seen from the integrated-signal plot (PEY-XA spectrum) shown in the inset of Figure 6; here, we also show the PEY-XA spectrum of neat water for comparison. These spectra were obtained in the same way as described for Figure 2.

At a sufficiently low photon energy, 530.5 eV (bottom spectrum), we essentially obtain the off-resonant PE spectrum of water; solute features are small (compare with Figure 1A). Increase of the photon energy to 532 eV results in considerable signal enhancement in the 25−30 eV BE region. There is no enhancement from neat water at this photon energy. Signal must thus be due to electron emission from water molecules directly interacting with Fe^{3+}. The Auger character of the evolving spectral feature can be indeed inferred from comparison with the resonant Auger spectra from bulk water, which occur at almost the same kinetic energies. Spectator-Auger contributions from (bulk) water Auger electrons quickly dominate the spectra once photon energies approach the bulk-water pre-edge. This is causing the sudden intensity rise at 534 eV photon energy. As far as the valence-band emission region of the resonant PE at 532 eV excitation energy is concerned, it is important to note that the spectral features do not exhibit any significant changes as compared to the off resonant emission; specifically, there is no resonant enhancement of any non-water related features observed. The lack of an obvious resonant enhancement of the Fe-derived 3d-states in resonant photoemission at the oxygen edge clearly indicates that screening of the O1s core-hole does not seem to involve Fe states to a large extent. These results are at odds with a recent interpretation of $L_{3,2}$-edge TFY spectra from $FeCl_3$ aqueous solutions.[36]

It remains to be clarified how the O1s excited states of coordinated water (i.e., the first-shell water molecules) relate to the Fe2p excited states discussed before. For that purpose, we plot all relevant energies on the same energy scale, and we chose core-level binding energies as zero energy; see Figure 7. The ionized core-level states, Fe^{3+} 2p and O1s, created upon resonant excitation (711 and 709 eV for Fe2p, and 532 eV for O1s of coordinating H_2O), are then to be compared to the energies of the neutral core-excited states. These are found to differ by 2-3 eV, suggesting that different valence electron configurations are probed, as expected for excitations strongly localized at either the iron or the water-oxygen site. This is also supported by the differences observed in the RPE spectra. To improve on this qualitative picture, a detailed theoretical description of the nature of orbital mixing in the excited state would be needed. Qualitatively, one expects considerable interaction of iron 3d with the unoccupied water $4a_1$ orbital, and it is reasonable that the energy of the latter is also affected by the missing water electron in L configurations.

We conclude this section by pointing out how we can use RPE spectroscopy for the quantitative determination of changes in the composition of the first solvation shell, and here we refer to the substitution of water molecules by the counteranion, that is, Cl^- in the current case. On the basis of our accompanying UV−vis measurements, and from comparison with reported speciation,[19] we estimate that the prevailing complex at 0.5 *m* concentration is $[Fe(H_2O)_5Cl]^{2+}$, followed by $[Fe(H_2O)_4Cl_2]^+$. At 1.5 *m*, the $[Fe(H_2O)_4Cl_2]^+$ complex dominates, followed by approximately equal amounts of $[Fe(H_2O)_5Cl]^{2+}$ and $[Fe(H_2O)_3Cl_3]$. Differences in the relative amount of Cl^- in the first solvation shell as a function of concentrations are found to be quantitatively reflected in our measurements through the varying 2p RPE signal enhancement. Specifically, the ratio of valence-signal enhancement for two different concentrations c_1, c_2 ($c_2 > c_1$) were observed to scale reasonably well with a factor $(c_2 - c_1)/n$, where n is the expected ratio of coordinated waters at the respective concentration. This is demonstrated in Supporting Information Figure SI1, comparing Fe2p RPE spectra from 0.5 and 1.5 *m* $FeCl_3$ concentrations.

There is no indication of spectral shifts of the resonantly enhanced features as a function of concentration, which rules out any strong effects of Cl^- on the electronic-structure interaction of the iron cation with the water molecules in the first solvation shell. The good quantitative agreement between total resonance-enhanced signal and speciation change also shows that resonant contributions from $Fe_3^+-Cl^-$ interactions are either absent or weak. Our finding is consistent with a previous O1s total-electron-yield XA measurement from Fe^{3+} aqueous solutions,[37] where small speciation-induced shifts of the pre-pre absorption-peak were observed to arise primarily from the direct interaction of water with Cl^- rather than from altered iron−water interaction. Our O1s RPE spectra of Figure 6 lead us to a similar conclusion because the signal near 532 eV is exclusively due to coordinated water, as evidenced by the characteristic water Auger-electron emission.

CONCLUSIONS

Experimental RPE spectra from a TM aqueous solution are reported, exemplified here for Fe^{3+}. Iron 2p and oxygen 1s valence RPE spectra from $FeCl_3$ aqueous solution provide previously inaccessible information on the electronic structure and interactions of the $Fe^{3+}(aq)$ cation with its surrounding water molecules. Specifically, through a combination of on- and off-resonant PE spectroscopy measurements, we not only identify electron configurations that reflect the ground-state orbital mixing, we also, very directly, observe the ultrafast electronic relaxation that leads to water-to-cation charge transfer for the 2p core-excited $Fe^{3+}(aq)$ complex. There seems to be less charge transfer in solution than in iron oxide, which is likely connected with the stabilization of water−water hydrogen bonds. It is noteworthy to emphasize that the transient charge-transfer channel, occurring in the presence of a core hole, has no analogue in optical excitation, and we would also like to point out that the present study does not probe Fe(III) to Fe(II) reduction.

We have also demonstrated the sensitivity of RPE spectroscopy for selectively investigating the water molecules in the first hydration shell. Moreover, by connecting measured valence and core electron binding energies with iron $L_{3,2}$ and O1s absorption energies, we experimentally assign the origin of the respective X-ray absorption transitions. Related to that, we have demonstrated that RPE spectroscopy readily provides the information required for an unambiguous interpretation of PEY-XA spectra from solution. In future studies, simultaneous recording of RPE and fluorescence-yield XA or X-ray emission spectra from TM aqueous solutions will allow for the unambiguous tracking of the charge-transfer mechanisms. Direct comparison of the fluorescence decay and the corresponding, much faster and far more probable, nonradiative decay channel will shed light into the recently postulated dark fluorescence channels.[14,36] We are convinced that the present RPE spectroscopy work will impact future extended experimental investigations on the electronic structure of first-row transition metal aqueous solutions. This will include the study of biologically relevant TM complexes in water as well as of fundamental processes in the broader context of X-ray radiation chemistry. Hopefully, experimental progress will be concurrently backed by advancing theory.

ASSOCIATED CONTENT

Supporting Information. Comparison of Fe2p RPE spectra from 0.5 and 1.5 *m* $FeCl_3$ concentrations. This material is available free of charge via the Internet at http://pubs.acs.org.

AUTHOR INFORMATION

Corresponding Author
bernd.winter@helmholtz-berlin.de

ACKNOWLEDGMENT

B.W. thanks the Deutsche Forschungsgemeinschaft (Project WI 1327/3-1) for support. S.E.B. acknowledges support from the U.S. National Science Foundation under contract CHE-0957869. We thank Manfred Faubel for insightful discussion, and assistance from the BESSY staff is gratefully acknowledged.

REFERENCES

(1) Evans, M. G.; Uri, N. *Nature* **1949**, *164*, 404.
(2) Nilsson, A.; Guo, J. *J. Electron Spectrosc. Relat. Phenom.* **2010**, *177*, 59–211.
(3) Moens, J.; Seidel, R.; Geerlings, P.; Faubel, M.; Winter, B.; Blumberger, J. *J. Phys. Chem. B* **2010**, *114*, 9173.
(4) Seidel, R.; Faubel, M.; Winter, B.; Blumberger, J. *J. Am. Chem. Soc.* **2009**, *131*, 16127.
(5) Seidel, R.; Thürmer, S.; Winter, B. *Phys. Chem. Lett.* **2011**, *2*, 633.
(6) Winter, B.; Faubel, M. *Chem. Rev.* **2006**, *106*, 1176.
(7) Winter, B. *Nucl. Instrum. Methods Phys. Res., Sect. A* **2009**, *601*, 139.
(8) *Core Level Spectroscopy of Solids*; de Groot, F., Kotani, A., Eds.; CRC Press: Boca Raton, FL, London, New York, 2008.
(9) Hüfner, S. *Photoelectron Spectroscopy: Principles and Applications*; Springer-Verlag: Berlin, Heidelberg, New York, London, Paris, Tokyo, Hong Kong, Barcelona, Budapest, 1995.
(10) Tanaka, A.; Takeao, J. *J. Phys. Soc. Jpn.* **1994**, *63*, 2788.
(11) Eberhardt, W.; Plummer, E. W.; Chen, C. T.; Ford, W. K. *Aust. J. Phys.* **1986**, *39*, 853.
(12) Stöhr, J. *NEXAFS Spectroscopy*; Springer Verlag: Berlin, 1992.
(13) Ohno, M.; van Riessen, G. A. *J. Electron Spectrosc. Relat. Phenom.* **2003**, *128*, 1.
(14) Nilsson, A. *Nat. Chem.* **2010**, *2*, 800.
(15) de Groot, F. M. F.; Arrio, M. A.; Sainctavit, P.; Cartier, C.; Chen, C. T. *Solid State Commun.* **1994**, *92*, 991.
(16) Suljoti, E.; de Groot, F. M. F.; Nagasono, M.; Glatzel, P.; Hennies, F.; Deppe, M.; Pietzsch, A.; Sonntag, B.; Föhlisch, A.; Wurth, W. *Phys. Rev. Lett.* **2009**, *103*, 137401.
(17) Winter, B.; Weber, R.; Widdra, W.; Dittmar, M.; Faubel, M.; Hertel, I. V. *J. Phys. Chem. A* **2004**, *108*, 2625.
(18) Cotton, F. A.; Wilkinson, G.; Murillo, C. A.; Bochmann, M. *Advanced Inorganic Chemistry*, 6th ed.; John Wiley & Sons: New York, Chichester, Weinheim, Brisbane, Singapore, Toronto, 1999.
(19) Liu, W.; Etschmann, B.; Brugger, J.; Spiccia, L.; Foran, G.; McInnes, B. *Chem. Geol.* **2006**, *231*, 326.
(20) Jorgensen, C. K. *Acta Chem. Scand.* **1954**, *8*, 1502.
(21) Winter, B.; Weber, R.; Hertel, I. V.; Faubel, M.; Jungwirth, P.; Brown, E. C.; Bradforth, S. E. *J. Am. Chem. Soc.* **2005**, *127*, 7203.
(22) Winter, B.; Aziz, E. F.; Ottosson, N.; Faubel, M.; Kosugi, N.; Hertel, I. V. *J. Am. Chem. Soc.* **2008**, *130*, 7130.
(23) Davis, L. C. *J. Appl. Phys.* **1986**, *59*, R25.
(24) Fujimori, A.; Saeki, M.; Kimizuka, N.; Taniguchi, M.; Suga, S. *Phys. Rev. B* **1986**, *34*, 7318.
(25) Droubay, T.; Chambers, S. A. *Phys. Rev. B* **2001**, *64*, 205414.
(26) Winter, B.; Aziz, E. F.; Hergenhahn, U.; Faubel, M.; Hertel, I. V. *J. Chem. Phys.* **2007**, *126*, 124504.
(27) de Groot, F. M. F.; Glatzel, P.; Bergmann, U.; van Aken, P. A.; Barrea, R. A.; Klemme, S.; Havecker, M.; Knop-Gericke, A.; Heijboer, W. M.; Weckhuysen, B. M. *J. Phys. Chem. B* **2005**, *109*, 20751.
(28) Yeh, J.-J. *Atomic Calculations of Photoionization Cross Sections and Asymmetry Parameters*; Gordon and Breach: Langhorne, PA, 1993.
(29) Ottosson, N.; Faubel, M.; Bradforth, S. E.; Jungwirth, P.; Winter, B. *J. Electron Spectrosc. Relat. Phenom.* **2010**, *177*, 60.

(30) Westre, T. E.; Kennepohl, P.; DeWitt, J. G.; Hedman, B.; Hodgson, K. O.; Solomon, E. I. *J. Am. Chem. Soc.* **1997**, *119*, 6297.
(31) Wasinger, E. C.; de Groot, F. M. F.; Hedman, B.; Hodgson, K. O.; Solomon, E. I. *J. Am. Chem. Soc.* **2003**, *125*, 12894.
(32) Chen, J.; Huang, D. J.; Tanaka, A.; Chang, C. F.; Chung, S. C.; Wu, W. B.; Chen, C. T. *Phys. Rev. B* **2004**, *69*, 085107.
(33) Tjeng, L. H.; Chen, C. T.; Ghijsen, J.; Rudolf, P.; Sette, F. *Phys. Rev. Lett.* **1991**, *67*, 501.
(34) Weinelt, M.; Nilsson, A.; Magnuson, M.; Wiell, T.; Wassdahl, N.; Karis, O.; Föhlisch, A.; Martensson, N.; Stöhr, J.; Samant, M. *Phys. Rev. Lett.* **1997**, *78*, 967.
(35) Hüfner, S.; Yang, S. H.; Mun, B. S.; Fadley, C. S.; Schafer, J.; Rotenberg, E.; Kevan, S. D. *Phys. Rev. B* **2000**, *61*, 12582.
(36) Aziz, A.; Chergui, M. *Nat. Chem.* **2010**, *2*, 853.
(37) Näslund, L. A.; Cavalleri, M.; Ogasawara, H.; Nilsson, A.; Pettersson, L. G. M.; Wernet, P.; Edwards, D. C.; Sandstrom, M.; Myneni, S. *J. Phys. Chem. A* **2003**, *107*, 6869.
(38) Zimmermann, R.; Steiner, P.; Claessen, R.; Reinert, F.; Hüfner, S.; Blaha, P.; Dufek, P. *J. Phys.: Condens. Matter* **1999**, *11*, 1657.